Photocatalytic Activation of Aryl(trifluoromethyl) Diazos to Carbenes for High-Resolution Protein Labeling with Red Light

David C. Cabanero,‡ Stavros K. Kariofillis,‡ Andrew C. Johns, Jinwoo Kim, Dann L. Parker, Jr., Carlo Ramil, Xavier Roy, Neel H. Shah,* and Tomislav Rovis*

ABSTRACT: State-of-the-art methods in photo-proximity labeling center on the targeted generation and capture of short-lived reactive intermediates to provide a snapshot of local protein environments. Diazirines are the current gold standard for high-resolution proximity labelling, generating short-lived aryl(trifluoromethyl) carbenes. Here, we present a method to access aryl(trifluoromethyl) carbenes from a stable diazo source *via* tissue penetrable, deep red (DR) to near-infrared (NIR) light (600-800 nm). The operative mechanism of this activation involves Dexter energy transfer from photoexcited osmium(II) photocatalysts to the diazo, thus revealing an aryl(trifluoromethyl) carbene. The labeling preferences of the diazo probe with amino acids are studied, showing high reactivity towards heteroatom–H bonds. Upon synthesis of a biotinylated diazo probe, labeling studies are conducted on native proteins as well as proteins conjugated to the Os photocatalyst. Finally, we demonstrate that conjugation of a protein inhibitor to the photocatalyst also enables selective protein labeling in the presence of spectator proteins.

INTRODUCTION

Proximity labeling (PL) is a powerful approach to mapping cellular microenvironments and providing snapshots of the interactions between biomolecules.[1] Improved understanding of these interactions (e.g., protein–protein interactions) reveals spatial proteomic information, enables improved understanding of cellular processes, and guides the design of new therapeutics.[2,3] The development of novel PL methods requires the careful consideration of both the "antenna" (typically an enzyme) on the protein of interest and the reactive species formed by this antenna from an inert small molecule, which governs the labeling radius.[4,5] For proteins, the labeling radius of a given PL method is related to the half-life of the reactive intermediate generated upon reaction with the antenna and the identity of the capturing amino acid side chain.[6]

PL has revolutionized the study of transient protein–protein interactions due to its advantages in the covalent capture and enrichment, obviating purification steps that may disrupt the cellular microenviroment.[4,7,8] Enzymatic approaches, primarily ascorbate peroxidases (e.g., APEX[9] and SPPLAT[10]) and biotin ligases (e.g., BioID[11] and TurboID[12]),[13,14] rely on the generation of reactive species (phenoxy radicals or activated esters, respectively). These reactive intermediates possess relatively long half-lives (1 ms to 5 mins) and limited variety in side-chain reactivity (aromatic groups or lysines, respectively). As such, developing new methods to tighten the labeling radius will enable high-resolution mapping of local protein environments. At the same time, the ability to conduct PL processes with a stimulus that affords spatiotemporal control provides an even more accurate snapshot of the cellular microenvironment.

Reactive species formed through direct photolysis (e.g., carbenes and nitrenes) have been shown to have extremely short half-lives; however, direct photolysis requires cytotoxic UV light and results in unselective labeling.[15–17] Visible light photo-proximity labeling has emerged as a means to overcome these limitations as high energy, short-lived intermediates are generated and localized near proteins through the use of a photocatalyst antenna and a photocatalytically-activatable probe. Accordingly, spatiotemporal control is achieved as the reactive probe is generated only in the presence of a light stimulus. A seminal report from MacMillan and Merck in 2020 demonstrated that diazirines could undergo activation by an Ir photocatalyst under blue LED irradiation to reveal reactive carbenes (Figure 1A).[18] Inherently, photo-proximity labeling techniques require the inert small molecule to be stable upon direct photolysis, which can be mediated by avoiding UV light and moving to lower energy light. Given the advantages of using even lower energy light, specifically in the phototherapeutic window (λ > 650 nm), there has been a recent push to access

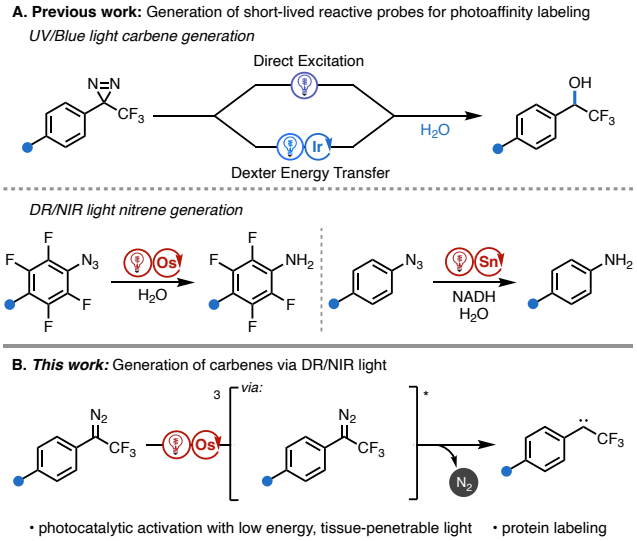

Figure 1. Generation of reactive probes for photo-proximity labeling.

https://doi.org/10.26434/chemrxiv-2023-pct8b **ORCID:** https://orcid.org/0000-0001-6287-8669

reactive probes under deep red (DR) or near-infrared (NIR) light.[19–21] Towards this aim, both our group[22] and the MacMillan lab[23] have reported that aryl azides can be activated with red light and Os or Sn photosensitizers, respectively, to reveal nitrenes or aminyl radicals (Figure 1B). These approaches have enabled extracellular spatiotemporal control in PL under red light irradiation.

Nitrenes[22] have a relatively long half-life compared to carbenes,[18] which results in a less tight labeling radius and a broader coverage of the microenvironment. Herein, we report a method to generate short-lived aryl(trifluoromethyl) carbenes with DR/NIR light from the analogous diazo compound, where an Os(II) polypyridyl photocatalyst, upon excitation by DR/NIR light, catalyzes carbene generation by energy transfer to the parent diazo compound (Figure 1C).

Diazo compounds have been used successfully in protein labeling via divergent activation modes.[24,25] Raines and coworkers have developed a suite of bioreversible esterification methods. These elegant modifications take place under mildly acidic pH (5.5 – 6.5), temporarily modulating the properties of the protein to effect a desired outcome (e.g., enhancing cellular uptake).[26–29] Metallopeptide approaches have also been applied, particularly with substituted dirhodium catalysts, to access carbenoid reactivity from diazo precursors.[30,31] These strategies are all highly enabling and address a variety of biological problems. Nevertheless, for proximity labeling, carbene generation is desired for its extremely short lifetime and promiscuous reactivity with many amino acid side chains.[32] Indeed, several studies have investigated the mechanism of diazirine decomposition and decoupled direct carbene reactivity from diazo-derived reactions.[33,34]

UV and blue light have been used to activate diazos to carbenes, but translation to proteins has lagged due to issues related to tissue penetration and photocytoxicity.[35] Notably, Dai and Yang found that by linking the diazo group to an extended π system, diazocoumarins can be activated via direct irradiation with blue LEDs or with a two-photon process using a near-infrared laser.[36] However, to access carbene reactivity for tightly localized protein labeling with low energy, tissue penetrable light, a photocatalytic method must be developed.

METHOD OPTIMIZATION AND MECHANISTIC STUDY

With the goal of gaining access to carbenes under red light irradiation, we first interrogated other carbene precursors because the prototypical aryl(trifluoromethyl) diazirines used for blue light-mediated proximity labeling require sensitization from high triplet energy photocatalysts. The required triplet energies, such as that of $[Ir(dFCF_3ppy)_2(dtbbpy)][PF_6]$ derivatives ($E^{T1}_{0,0}$ ~2.6 eV), to achieve this chemistry are too high to be reached with low energy DR/NIR light: 660 nm is only approximately 1.88 eV. In some cases, it is invoked that diazirines isomerize into diazos prior to loss of dinitrogen, and so we reasoned that the barrier to activate aryl(trifluoromethyl) diazo compounds should be lower than diazirines.[33,34] Indeed, using 1 mol% $[Os(Me_4phen)_3][Cl]_2$ (**Os1**) as a photocatalyst,[37,38] the O–H insertion of diazo **D2** into methanol proceeds in 95% yield to afford **2** (Table 1, Entry 1). Decreasing

Table 1. Reaction Evaluation for O–H Insertion.

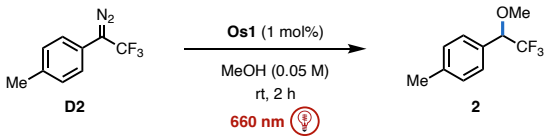

Entry	Deviation from Standard Conditions	% Yield[a]
1	none	95%
2	0.5 mol% **Os1**	95%
3	0.1 mol% **Os1**	39%
4	740 nm LEDs	30%
5	740 nm LEDs, 24 h	87%
6	without 660 nm LEDs	0%[b]
7	without **Os1**	0%[b]

[a] ^{19}F NMR yield with 1-fluoronaphthalene as external standard. [b] 100% diazo remaining.

the Os loading to 0.5 mol% and 0.1 mol% affords the O–H insertion product **2** in 95% and 39% yield, respectively (Table 1, Entries 2-3). Furthermore, using a NIR LED (740 nm) in place of the 660 nm LED produces **2** in 30% yield (Table 1, Entry 4), demonstrating that even lower energy wavelengths are amenable to the transformation. When the reaction is run for 24 hours under 740 nm LEDs, 87% yield of the product can be obtained (Table 1, Entry 5). Importantly, control studies indicate that the reaction requires both light and the Os catalyst for any conversion of the diazo (Table 1, Entries 6-7).

Cyclic voltammetry of diazo **D2** showed an irreversible reduction at $E_{1/2}$ = –1.35 V vs Ag/AgCl in MeCN. Thus, the excited state of **Os1** ($E_{1/2}$ = –1.25 V vs Ag/AgCl in MeCN) is

Table 2. Photocatalyst Evaluation.

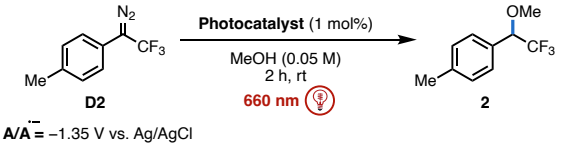

A/A$^{\cdot-}$ = –1.35 V vs. Ag/AgCl

Entry	Photocatalyst	$E_{1/2}(Os^{II*}/Os^{III})$[a]	E_T (eV)	Yield (%)[b]
1	**Os1**	–1.22	1.81	95%
2	**$[Os(dFCF_3Ph\text{-}pypm)_2][Cl]_2$**	–0.62	1.80	17%[c]
3	**$[Os(dFCF_3Ph\text{-}pypm)_2][Cl]_2$** no light	–0.62	1.80	0%[d]

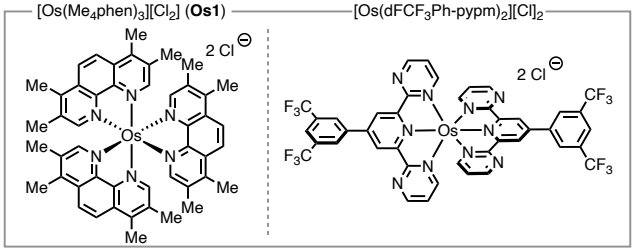

Reactions run on 0.03 mmol scale. [a] V vs Ag/AgCl in MeCN. [b] ^{19}F NMR yield with 1,3,5-trifluorobenzene as external standard. [c] 74% diazo remaining. [d] 100% diazo remaining.

unlikely to enable single electron reduction of the diazo, implicating an energy transfer mechanism. To further corroborate this, we employed a different Os photocatalyst, $[Os(dFCF_3Ph\text{-}pypm)_2][Cl]_2$, which has a similarly high triplet energy (1.80 eV) as **Os1** but is insufficiently reducing in its excited state ($E_{1/2}$ = –0.62 V vs Ag/AgCl in MeCN). Although **Os1** is a more efficient catalyst, decomposition of **D2** is indeed observed with $[Os(dFCF_3Ph\text{-}pypm)_2][Cl]_2$ (Table 2, Entry 2), affording **2** in 17% yield. This finding suggests that the mechanism to carbene formation is Dexter energy transfer from the excited state of the Os(II) photocatalyst to the diazo. Subsequent, rapid loss of N_2 thus forms the carbene.

Next, we conducted a computational study to examine the feasibility of carbene generation via energy transfer. First, we found that the diazo could be activated by the photocatalyst via energy transfer with a calculated triplet energy of at least ~27 kcal mol^{-1} (triplet energy of **Os1** ~42 kcal mol^{-1}).[39] It was also determined that the diazo decomposition from its triplet excited state has a relatively low barrier of approximately 8.46 kcal mol^{-1}. To further corroborate the energy transfer mechanism, a Hammett plot was generated, exhibiting no dependence on the arene electronics (*p*-CF_3 to *p*-OMe) to the rate of diazo decomposition (see SI, Figure S3). If an *Os(II)-catalyzed reduction of the diazo was operative, we would expect the diazo electronics to influence the rate of substrate decomposition. Taken together, these studies lead us to believe the diazo undergoes Dexter energy transfer from *Os(II) to form the carbene.

SYNTHETIC APPLICATIONS

We subsequently investigated O–H insertion reactions in alcohol solvent with respect to the electronics of the differing *para*-substituents on the diazo. Specifically, these studies could guide us to design the most reactive diazo probe for biological studies. A clear trend was observed that electron-neutral to -rich diazos produce higher yields in the O–H insertion of methanol than their electron poor derivatives (Figure 2A). The *para*-methoxy and *para*-methyl diazo compounds yield O–H insertion products **1** and **2**, respectively, in excellent yields. Conversely, the *para*-methyl ester-substituted diazo affords **6** in only 6% yield. It is important to note that full starting material conversion is obtained in all cases, suggesting that the discrepancy in yields is not from the rate of decomposition (to which there is no relationship, as per the Hammett study) but from the character of the resulting carbene species. For example, the aryl(trifluoromethyl) diazos possessing a *para*-bromo or *para*-methyl ester group produce dimeric species and their isomers upon carbene generation.[40,41] These results suggest that the electron-rich diazos yield singlet carbenes while the electron-poor diazos yield triplet carbenes, as the diradical character of triplet carbenes would disfavor O–H insertion, a finding consistent with a recent computational study by Wulff using aryl diazirines.[42]

We also sought to examine the tolerance of the photocatalytic reaction with bioorthogonal functional groups (Figure 2B). Accordingly, we functionalized the *p*-tolyl(trifluoromethyl) diazo to prepare an electron-neutral, biotinylated derivative. When applied to the O–H insertion conditions, this compound affords **7** in a 50% isolated yield. Furthermore,

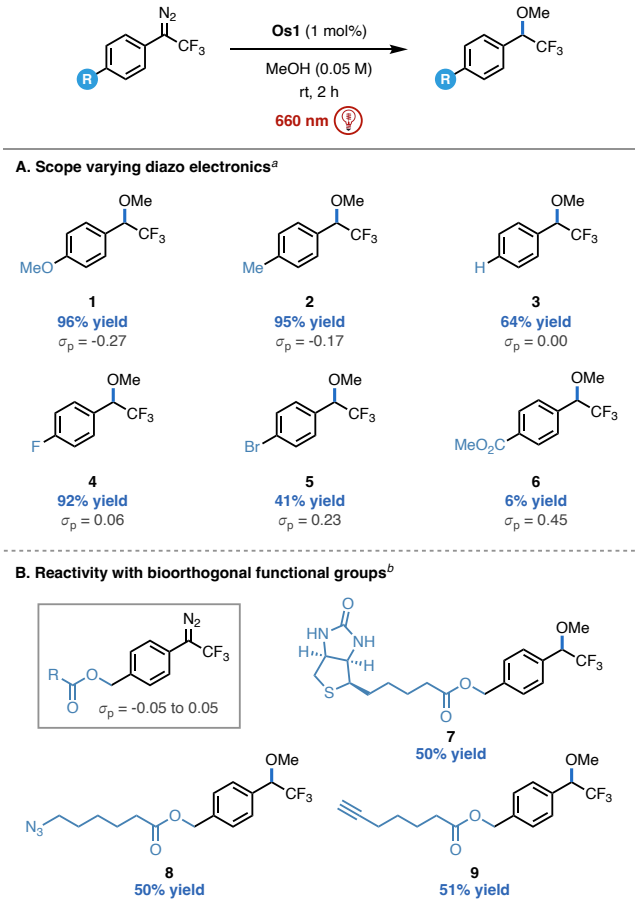

Figure 2. Scope of diazos for O–H insertion. Reactions were performed on 0.1 mmol scale. [a] ^{19}F NMR yields using 1-fluoronaphthalene as an external standard. [b] 0.05 mmol scale reaction.

azidated and alkynylated aryl(trifluoromethyl) diazo compounds produce **8** and **9**, respectively, in good yields. Thus, these derivatized aryl(trifluoromethyl) diazo compounds undergo O–H insertions in good yields and with high functional group tolerance under the photocatalytic conditions.

The O–H insertion study demonstrated that electron-rich and -neutral substituents reveal carbenes most efficiently for reaction with methanol. In light of these results, we initiated reactivity studies using the *p*-tolyl-derived diazo, which possesses a benzylic position for synthesizing a probe for biological studies. Before pursuing protein labeling studies, the reactivity of various amino acids was studied with the *p*-tolyl(trifluoromethyl) diazo (Figure 3A). To isolate the reactivity of the side chain, the *N*- and *C*- termini of the amino acid substrates were protected. In a reaction with Cys, the S–H insertion proceeds in 59% yield to afford **10**. Other polar, nucleophilic residues, including the aliphatic alcohols of Ser (**11**) and Thr (**12**) undergo high yielding O–H insertion. These studies are indicative of high labeling preference for polar amino acids that are expectedly surface exposed on proteins. It was also observed that O–H insertion proceeds on the aromatic alcohol of tyrosine to yield **13** in 44% yield.

Acidic amino acids such as Asp and Glu had the highest insertion yields, producing **14** and **15** in 89% and 84% yields, respectively. Additionally, N–H insertion proceeds with Gln (50% yield, **16**) and His (25% yield, **17**). However,

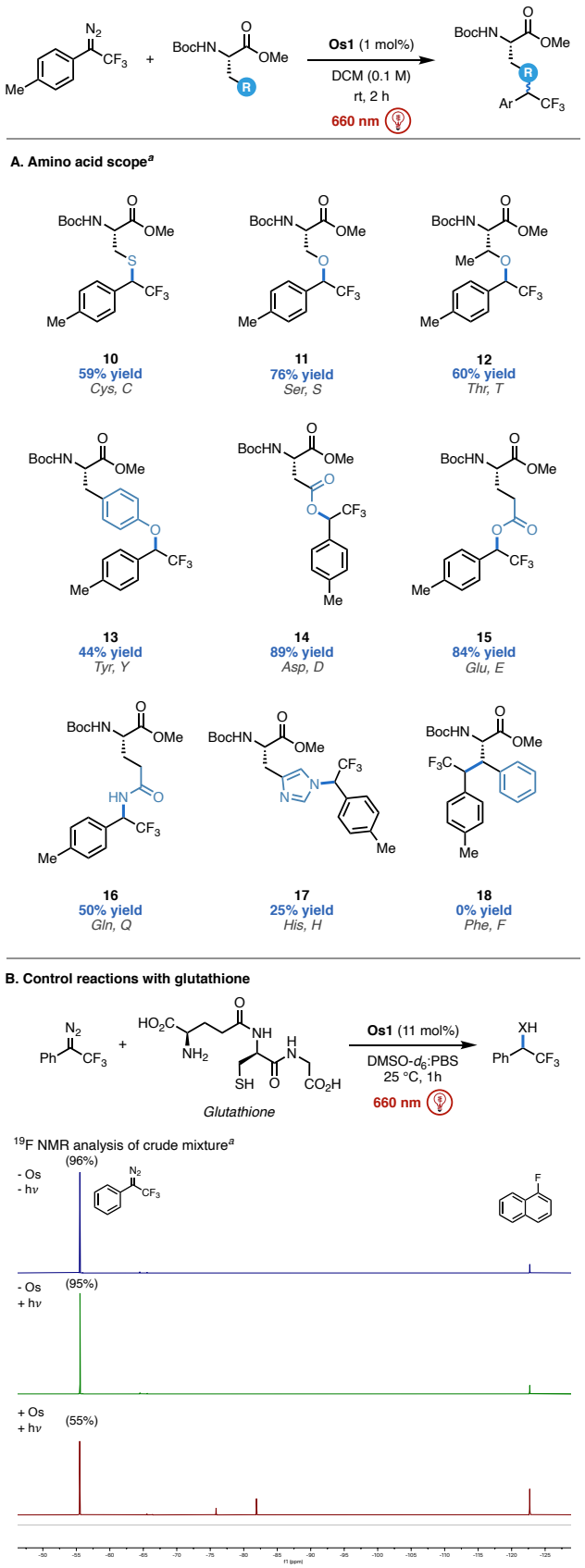

Figure 3. Labeling preferences of amino acids. [a] ^{19}F NMR yields using 1-fluoronaphthalene as external standard.

C–H insertion into Phe was not observed to produce **18**; instead, probe dimers and other decomposition products were observed (Figure 3A).

Notably, the amino acid labeling reactions are conducted in dichloromethane, where carboxylic acids are expected to be protonated. As such, background reactivity is observed for the O–H insertion into Glu in DCM under 660 nm LED irradiation (84% with Os; 11% without Os) as a result of a protonation-substitution event, akin to the reaction between (trimethylsilyl)diazomethane and a carboxylic acid.[43] These results are consistent with diazo-mediated bioreversible esterification strategies reported by Raines.[26–29] However, at physiological pH, carboxylic acids are expectedly deprotonated in aqueous solution, thus the acidic decomposition of diazos is unlikely to be competitive with our photocatalytic system. To interrogate this, we treated our substrate with glutathione (reduced), which not only contains two free carboxylic acids, an amine, and a thiol, but is also present in relatively high concentrations in cells. In a PBS/DMSO mixture, the diazo does not decompose in the presence of glutathione without Os when irradiated (Figure 3B). It is not until both catalyst and light are present that diazo decomposition is observed, which offers great promise that background, non-targeted labeling will be minimal in protein studies.

PROTEIN LABELING

To demonstrate that our technology is translatable to protein labeling, we synthesized PEGylated and biotinylated diazo probes **D10** and **D11**, which differ only by their linkage identity — ester (**D10**) or amide (**D11**). The syntheses start from commercially available 2,2,2-trifluoro-1-(*p*-tolyl)ethan-1-one and are scalable (see SI, Section IX for full synthetic details). To validate the utility of the diazo probes, we performed *in vitro* labeling of carbonic anhydrase (CA) with **Os-1** and diazo **D10** under 660 nm irradiation and observed robust biotinylation of CA only when our Osmium catalyst was present (Figure 4A).

Next, we evaluated diazo-based protein labeling at different light wavelengths while also comparing the efficacy of the diazo probe **D11** to its diazirine counterpart **Dz1** (Figure 4B).[18] Under UV (370 nm) irradiation, both the diazo and the diazirine label bovine serum albumin (BSA). Under blue light (456 nm), the diazirine is untouched in the absence of Ir, consistent with MacMillan's report.[18] On the other hand, the diazo probe is photoactive under blue light irradiation, as non-catalytic protein labeling of BSA is observed. This observation is consistent with several recent reports of diazo compound activation using blue LEDs for synthetic transformations.[44–46] Thus, unlike aryl(trifluoromethyl) diazirine sensitization, diazo probes are incompatible with blue light photocatalytic proximity labeling. However, when irradiated with deep red (660 nm) light, the diazo system labels BSA only when **Os1** is used. Furthermore, no photocatalytic activity is observed when employing the diazirine under red light irradiation with **Os1**, which suggests that a higher photocatalyst triplet energy is required for diazirine activation (e.g., [Ir(dFCF$_3$ppy)$_2$(dtbbpy)][PF$_6$] derivative ($E^{T1}_{0,0}$ ~2.6 eV) *versus* [Os(Me$_4$phen)$_3$][PF$_6$]$_2$ ($E^{T1}_{0,0}$ ~1.8 eV)).[38,47] These results suggest that we can generate carbenes catalytically using low energy, tissue-

https://doi.org/10.26434/chemrxiv-2023-pct8b **ORCID:** https://orcid.org/0000-0001-6287-8669

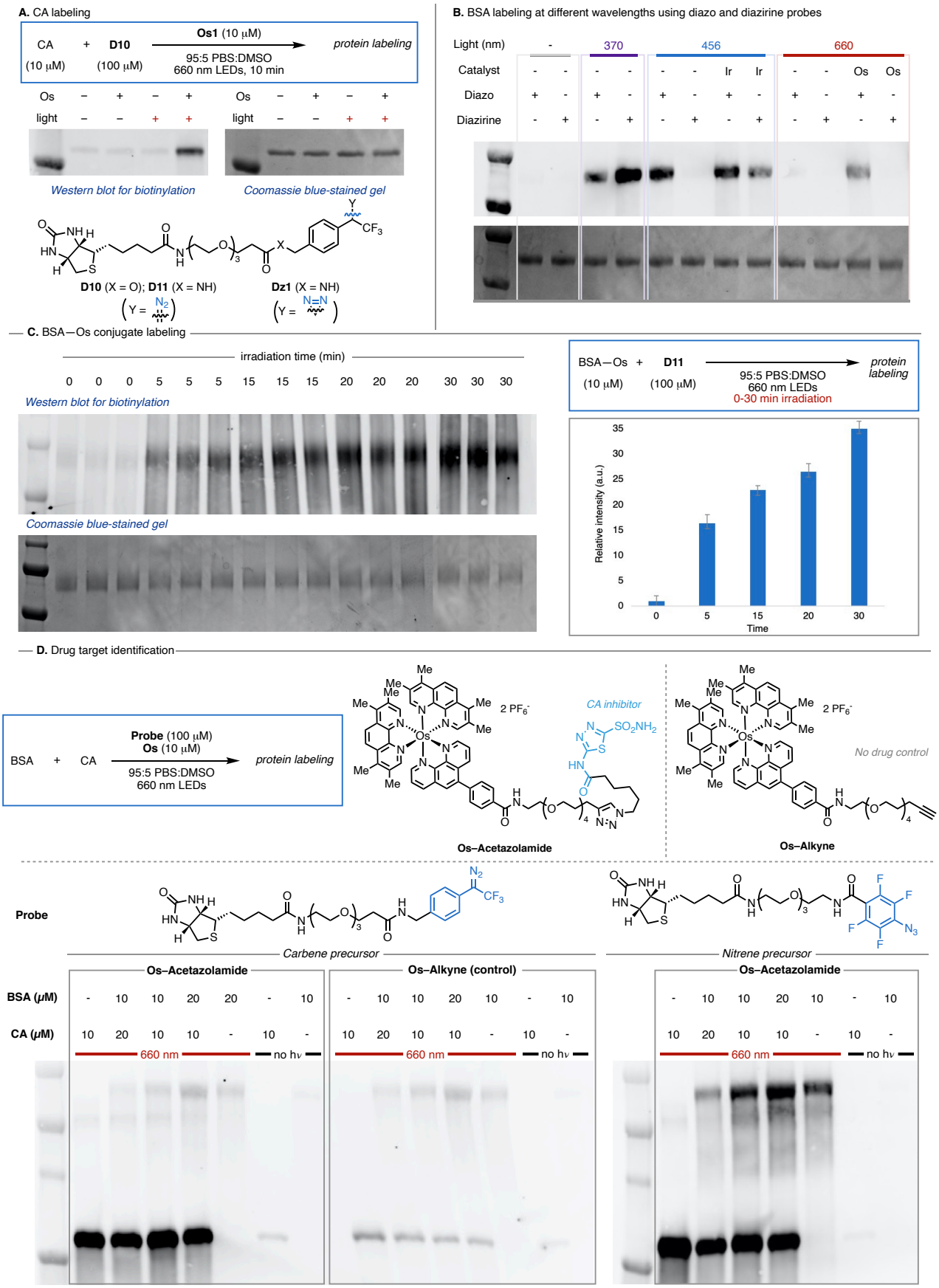

Figure 4. (a) Labeling of carbonic anhydrase (CA) and control studies. (b) Wavelength-dependent activation of diazo and diazirine probes. (c) Conjugation of **Os1** to bovine serum albumin (BSA) and time course. (d) Selective targeting of CA using an Os–Acetazolamide conjugate using diazo (left) and azide (right).

penetrable light, and we anticipate the orthogonal photoactivation profiles of diazos and diazirines can be harnessed for proximity labeling applications.

To model proximity between the photocatalyst and a target protein, we used Cu-catalyzed azide-alkyne cycloaddition (CuAAC) to conjugate azidated BSA to an Os photocatalyst bearing an alkyne. Upon 660 nm irradiation, more efficient labeling is observed when the Os catalyst is conjugated to BSA (i.e., in proximity) as opposed to free floating catalyst, consistent with our hypothesis that the generated carbene species would result in increased labeling of proximal proteins. Indeed, significant labeling of BSA is gradually observed over time (Figure 4C). Analogous studies with the Os photocatalyst conjugated to CA also demonstrate that labeling requires 660 nm LEDs and that increased labeling occurs with increased irradiation time (see SI, Figure S17).

To further this technology, we sought to target protein labeling via non-covalent interactions such as those found in target identification studies. Accordingly, we investigated the labeling of CA by conjugating the Os photocatalyst to acetazolamide, a diuretic medication and known CA inhibitor.[48,49] Higher biotinylation of CA with this acetazolamide-derived catalyst was achieved relative to **Os1** (Figure 4D). Introduction of BSA as a spectator protein, even at a 2:1 BSA:CA ratio, did not influence the protein labeling, as CA was still predominantly labeled. When the precursor to the acetazolamide-derived photocatalyst (that does not possess the inhibitor) is employed, roughly equal biotinylation of CA and BSA is observed. Control reactions confirmed that without conjugation to Os, the parent acetazolamide compound does not mediate any protein biotinylation. Furthermore, while the level of CA biotinylation decreases when employing a 10-fold excess of acetazolamide relative to Os–acetazolamide in a competition study, labeling of CA still dominates over BSA (see SI, Figure S23).

A primary motivation for the photocatalytic generation of carbenes under red light is to enable protein labeling within a tight radius. Satisfyingly, when comparing the labeling probe with our previously reported perfluorinated azide system,[22] promiscuous labeling is observed using the Os–acetazolamide conjugate, where both BSA and CA are labeled (1.5x increase in intensity for CA *versus* BSA) when using the nitrene precursor. In comparison, CA is much more selectively labeled when using the carbene precursor (17x increase in intensity for CA *versus* BSA). This is consistent with our hypothesis that the shorter lifetimes of carbenes relative to nitrenes should translate to a tighter labeling radius. More broadly, these studies demonstrate that our diazo-to-carbene strategy could map selective delivery of therapeutics to a druggable target under low energy light irradiation.[50]

CONCLUSION

In conclusion, we have developed a method for generating carbenes from aryl(trifluoromethyl) diazos under red light irradiation. Mechanistic studies reveal that Os(II) photoredox catalysts undergo energy transfer reactions with the parent diazo species to reveal carbenes. The reactivity of these diazos is demonstrated in O–H insertion reactions with methanol, revealing that electron-rich diazos are most reactive. Importantly, diazo activation requires both light and catalyst, and these diazos can be activated with even NIR (740 nm) light. Reactions with amino acids show that, upon activation, the diazos react efficiently with nucleophilic atoms through O–H, S–H, and N–H insertions.

When using a biotinylated diazo probe, protein labeling studies reveal that the diazo requires both light and photocatalyst for carbene generation. While UV and blue light can activate the diazo, we only achieve carbene access with red light in the presence of a photocatalyst. Conjugation of the Os catalyst to a protein results in enhanced biotinylation, and conjugation to a small-molecule protein inhibitor results in selective labeling in the presence of spectator proteins, thus revealing reactivity characteristics unique to carbenes. Taken together, this technology reveals, for the first time, the generation of extremely short-lived carbenes using low energy, tissue penetrable light. As such, we anticipate this tool will be highly useful for photo-proximity labeling and other chemical biology applications.

ASSOCIATED CONTENT

Supporting Information

The Supporting Information is available free of charge on the ACS Publications website.

Experimental procedures, spectroscopic data, uncropped Western blot images and Coomassie blue-stained gels, details of the computational study (PDF)

AUTHOR INFORMATION

Corresponding Author

Neel H. Shah – *Department of Chemistry, Columbia University, New York, NY 10027, United States. orcid: 0000-0002-1186-0626.*
Email: neel.shah@columbia.edu
Tomislav Rovis – *Department of Chemistry, Columbia University, New York, NY 10027, United States. orcid: 0000-0001-6287-8669.*
Email: tr2504@columbia.edu

Authors

David C. Cabanero – Department of Chemistry, Columbia University, New York, NY 10027, United States. orcid: 0000-0001-9148-7771.

Stavros K. Kariofillis – Department of Chemistry, Columbia University, New York, NY 10027, United States. orcid: 0000-0002-5461-3190

Andrew Johns – Department of Chemistry, Columbia University, New York, NY 10027, United States. orcid: 0000-0002-3197-1390.

Jinwoo Kim – Department of Chemistry, Columbia University, New York, NY 10027, United States.

Dann L. Parker, Jr. – Discovery Chemistry, Merck & Co., Inc., Rahway, NJ, 07065, United States.

Carlo Ramil – Discovery Chemistry, Merck & Co., Inc., Cambridge, MA 02141, United States.

Xavier Roy – Department of Chemistry, Columbia University, New York, NY 10027, United States.

Author Contributions

‡D.C.C. and S.K.K. contributed equally.

Funding Sources

ACKNOWLEDGMENT

T.R. thanks Merck Research Laboratories for partial support of this work. N.H.S. thanks the NIH (R35GM138014). D.C.C. acknowledges the Guthikonda family for a graduate fellowship. We thank Anne van Vlimmeren, Minhee Lee and Dr. Nicholas Tay for helpful discussions. Research reported pertaining to cryoprobe NMR data in this publication was supported by the Office of the Director of the NIH under Award Number S10OD026749.

REFERENCES

(1) Kang, M.-G.; Rhee, H.-W. Molecular Spatiomics by Proximity Labeling. *Acc. Chem. Res.* **2022**, *55*, 1411–1422.

(2) Ruffner, H.; Bauer, A.; Bouwmeester, T. Human Protein–Protein Interaction Networks and the Value for Drug Discovery. *Drug Discov. Today* **2007**, *12*, 709–716.

(3) Scott, D. E.; Bayly, A. R.; Abell, C.; Skidmore, J. Small Molecules, Big Targets: Drug Discovery Faces the Protein–Protein Interaction Challenge. *Nat. Rev. Drug Discov.* **2016**, *15*, 533–550.

(4) Qin, W.; Cho, K. F.; Cavanagh, P. E.; Ting, A. Y. Deciphering Molecular Interactions by Proximity Labeling. *Nat. Methods* **2021**, *18*, 133–143.

(5) Seath, C. P.; Trowbridge, A. D.; Muir, T. W.; MacMillan, D. W. C. Reactive Intermediates for Interactome Mapping. *Chem. Soc. Rev.* **2021**, *50*, 2911–2926.

(6) Oakley, J. V.; Buksh, B. F.; Fernández, D. F.; Oblinsky, D. G.; Seath, C. P.; Geri, J. B.; Scholes, G. D.; MacMillan, D. W. C. Radius Measurement via Super-Resolution Microscopy Enables the Development of a Variable Radii Proximity Labeling Platform. *Proc. Natl. Acad. Sci. U.S.A.* **2022**, *119*, e2203027119.

(7) Roux, K. J. Marked by Association: Techniques for Proximity-Dependent Labeling of Proteins in Eukaryotic Cells. *Cell. Mol. Life Sci.* **2013**, *70*, 3657–3664.

(8) Rao, V. S.; Srinivas, K.; Sujini, G. N.; Kumar, G. N. S. Protein-Protein Interaction Detection: Methods and Analysis. *Int. J. Proteomics* **2014**, *2014*, 1–12.

(9) Lam, S. S.; Martell, J. D.; Kamer, K. J.; Deerinck, T. J.; Ellisman, M. H.; Mootha, V. K.; Ting, A. Y. Directed Evolution of APEX2 for Electron Microscopy and Proximity Labeling. *Nat. Methods* **2015**, *12*, 51–54.

(10) Rees, J. S.; Li, X.; Perrett, S.; Lilley, K. S.; Jackson, A. P. Selective Proteomic Proximity Labeling Assay Using Tyramide (SPPLAT): A Quantitative Method for the Proteomic Analysis of Localized Membrane-Bound Protein Clusters. *Curr. Protoc. Protein Sci.* **2017**, *88*, 19.27.1-19.27.18.

(11) Roux, K. J.; Kim, D. I.; Burke, B.; May, D. G. BioID: A Screen for Protein-Protein Interactions. *Curr. Protoc. Protein Sci.* **2018**, *91*.

(12) Branon, T. C.; Bosch, J. A.; Sanchez, A. D.; Udeshi, N. D.; Svinkina, T.; Carr, S. A.; Feldman, J. L.; Perrimon, N.; Ting, A. Y. Efficient Proximity Labeling in Living Cells and Organisms with TurboID. *Nat. Biotechnol.* **2018**, *36*, 880–887.

(13) Rees, J. S.; Li, X.-W.; Perrett, S.; Lilley, K. S.; Jackson, A. P. Protein Neighbors and Proximity Proteomics. *Mol. Cell. Proteomics* **2015**, *14*, 2848–2856.

(14) Varnaitė, R.; MacNeill, S. A. Meet the Neighbors: Mapping Local Protein Interactomes by Proximity-Dependent Labeling with BioID. *Proteomics* **2016**, *16*, 2503–2518.

(15) Hashimoto, M.; Hatanaka, Y. Recent Progress in Diazirine-Based Photoaffinity Labeling. *Eur. J. Org. Chem.* **2008**, *2008*, 2513–2523.

(16) Kotzyba-Hibert, F.; Kapfer, I.; Goeldner, M. Recent Trends in Photoaffinity Labeling. *Angew. Chem. Int. Ed. Engl.* **1995**, *34*, 1296–1312.

(17) Dubinsky, L.; Krom, B. P.; Meijler, M. M. Diazirine Based Photoaffinity Labeling. *Bioorg. Med. Chem.* **2012**, *20*, 554–570.

(18) Geri, J. B.; Oakley, J. V.; Reyes-Robles, T.; Wang, T.; McCarver, S. J.; White, C. H.; Rodriguez-Rivera, F. P.; Parker, D. L.; Hett, E. C.; Fadeyi, O. O.; Oslund, R. C.; MacMillan, D. W. C. Microenvironment Mapping via Dexter Energy Transfer on Immune Cells. *Science* **2020**, *367*, 1091–1097.

(19) Beck, L. R.; Xie, K. A.; Goldschmid, S. L.; Kariofillis, S. K.; Joe, C. L.; Sherwood, T. C.; Sezen-Edmonds, M.; Rovis, T. Red-Shifting Blue Light Photoredox Catalysis for Organic Synthesis: A Graphical Review. *SynOpen* **2023**, *7*, 76–87.

(20) Ash, C.; Dubec, M.; Donne, K.; Bashford, T. Effect of Wavelength and Beam Width on Penetration in Light-Tissue Interaction Using Computational Methods. *Lasers Med. Sci.* **2017**, *32*, 1909–1918.

(21) Mei, L.; Veleta, J. M.; Gianetti, T. L. Helical Carbenium Ion: A Versatile Organic Photoredox Catalyst for Red-Light-Mediated Reactions. *J. Am. Chem. Soc.* **2020**, *142*, 12056–12061.

(22) Tay, N. E. S.; Ryu, K. A.; Weber, J. L.; Olow, A. K.; Cabanero, D. C.; Reichman, D. R.; Oslund, R. C.; Fadeyi, O. O.; Rovis, T. Targeted Activation in Localized Protein Environments via Deep Red Photoredox Catalysis. *Nat. Chem.* **2023**, *15*, 101–109.

(23) Buksh, B. F.; Knutson, S. D.; Oakley, J. V.; Bissonnette, N. B.; Oblinsky, D. G.; Schwoerer, M. P.; Seath, C. P.; Geri, J. B.; Rodriguez-Rivera, F. P.; Parker, D. L.; Scholes, G. D.; Ploss, A.; MacMillan, D. W. C. μMap-Red: Proximity Labeling by Red Light Photocatalysis. *J. Am. Chem. Soc.* **2022**, *144*, 6154–6162.

(24) Mix, K. A.; Aronoff, M. R.; Raines, R. T. Diazo Compounds: Versatile Tools for Chemical Biology. *ACS Chem. Biol.* **2016**, *11*, 3233–3244.

(25) Ollevier, T.; Carreras, V. Emerging Applications of Aryl Trifluoromethyl Diazoalkanes and Diazirines in Synthetic Transformations. *ACS Org. Inorg. Au* **2022**, *2*, 83–98.

(26) McGrath, N. A.; Andersen, K. A.; Davis, A. K. F.; Lomax, J. E.; Raines, R. T. Diazo Compounds for the Bioreversible Esterification of Proteins. *Chem. Sci.* **2015**, *6*, 752–755.

(27) Mix, K. A.; Lomax, J. E.; Raines, R. T. Cytosolic Delivery of Proteins by Bioreversible Esterification. *J. Am. Chem. Soc.* **2017**, *139*, 14396–14398.

(28) Ressler, V. T.; Mix, K. A.; Raines, R. T. Esterification Delivers a Functional Enzyme into a Human Cell. *ACS Chem. Biol.* **2019**, *14*, 599–602.

(29) Jun, J. V.; Petri, Y. D.; Erickson, L. W.; Raines, R. T. Modular Diazo Compound for the Bioreversible Late-Stage Modification of Proteins. *J. Am. Chem. Soc.* **2023**, *145*, 6615–6621.

(30) Antos, J. M.; Francis, M. B. Selective Tryptophan Modification with Rhodium Carbenoids in Aqueous Solution. *J. Am. Chem. Soc.* **2004**, *126*, 10256–10257.

(31) Ball, Z. T. Designing Enzyme-like Catalysts: A Rhodium(II) Metallopeptide Case Study. *Acc. Chem. Res.* **2013**, *46*, 560–570.

(32) Sigrist, H.; Mühlemann, M.; Dolder, M. Philicity of Amino Acid Side-Chains for Photogenerated Carbenes. *J. Photochem. Photobiol. B., Biol.* **1990**, *7*, 277–287.

(33) O'Brien, J. G. K.; Jemas, A.; Asare-Okai, P. N.; am Ende, C. W.; Fox, J. M. Probing the Mechanism of Photoaffinity

Labeling by Dialkyldiazirines through Bioorthogonal Capture of Diazoalkanes. *Org. Lett.* **2020**, *22*, 9415–9420.
(34) West, A. V.; Amako, Y.; Woo, C. M. Design and Evaluation of a Cyclobutane Diazirine Alkyne Tag for Photoaffinity Labeling in Cells. *J. Am. Chem. Soc.* **2022**, *144*, 21174–21183.
(35) Toh, K.; Nishio, K.; Nakagawa, R.; Egoshi, S.; Abo, M.; Perron, A.; Sato, S.; Okumura, N.; Koizumi, N.; Dodo, K.; Sodeoka, M.; Uesugi, M. Chemoproteomic Identification of Blue-Light-Damaged Proteins. *J. Am. Chem. Soc.* **2022**, *144*, 20171–20176.
(36) Dai, S.-Y.; Yang, D. A Visible and Near-Infrared Light Activatable Diazocoumarin Probe for Fluorogenic Protein Labeling in Living Cells. *J. Am. Chem. Soc.* **2020**, *142*, 17156–17166.
(37) Ravetz, B. D.; Tay, N. E. S.; Joe, C. L.; Sezen-Edmonds, M.; Schmidt, M. A.; Tan, Y.; Janey, J. M.; Eastgate, M. D.; Rovis, T. Development of a Platform for Near-Infrared Photoredox Catalysis. *ACS Cent. Sci.* **2020**, *6*, 2053–2059.
(38) Goldschmid, S. L.; Bednářová, E.; Beck, L. R.; Xie, K.; Tay, N. E. S.; Ravetz, B. D.; Li, J.; Joe, C. L.; Rovis, T. Tuning the Electrochemical and Photophysical Properties of Osmium-Based Photoredox Catalysts. *Synlett* **2022**, *33*, 247–258.
(39) Note that this theoretical triplet energy may be an underestimate; there has been debate on the accuracy of organic biradical systems using DFT computation. See: Shee, J.; Arthur, E. J.; Zhang, S.; Reichman, D. R.; Friesner, R. A. Singlet–Triplet Energy Gaps of Organic Biradicals and Polyacenes with Auxiliary-Field Quantum Monte Carlo. *J. Chem. Theory Comput.* **2019**, *15*, 4924–4932.
(40) Regitz, M.; Maas, G. Thermal Properties. In *Diazo Compounds*; Elsevier, 1986; pp 65–95. https://doi.org/10.1016/B978-0-12-585840-3.50006-4.
(41) Doyle, M. P.; Devia, A. H.; Bassett, K. E.; Terpstra, J. W.; Mahapatro, S. N. Unsymmetrical Alkenes by Carbene Coupling from Diazirine Decomposition in the Presence of Diazo Compounds. *J. Org. Chem.* **1987**, *52*, 1619–1621.
(42) Musolino, S. F.; Pei, Z.; Bi, L.; DiLabio, G. A.; Wulff, J. E. Structure–Function Relationships in Aryl Diazirines Reveal Optimal Design Features to Maximize C–H Insertion. *Chem. Sci.* **2021**, *12*, 12138–12148.
(43) Kühnel, E.; Laffan, D. D. P.; Lloyd-Jones, G. C.; Martínez del Campo, T.; Shepperson, I. R.; Slaughter, J. L. Mechanism of Methyl Esterification of Carboxylic Acids by Trimethylsilyldiazomethane. *Angew. Chem., Int. Ed.* **2007**, *46*, 7075–7078.
(44) Jurberg, I. D.; Davies, H. M. L. Blue Light-Promoted Photolysis of Aryldiazoacetates. *Chem. Sci.* **2018**, *9*, 5112–5118.
(45) Durka, J.; Turkowska, J.; Gryko, D. Lightening Diazo Compounds? *ACS Sustain. Chem. Eng.* **2021**, *9*, 8895–8918.
(46) Yang, Z.; Stivanin, M. L.; Jurberg, I. D.; Koenigs, R. M. Visible Light-Promoted Reactions with Diazo Compounds: A Mild and Practical Strategy Towards Free Carbene Intermediates. *Chem. Soc. Rev.* **2020**, *49*, 6833–6847.
(47) Lowry, M. S.; Goldsmith, J. I.; Slinker, J. D.; Rohl, R.; Pascal, R. A.; Malliaras, G. G.; Bernhard, S. Single-Layer Electroluminescent Devices and Photoinduced Hydrogen Production from an Ionic Iridium(III) Complex. *Chem. Mater.* **2005**, *17*, 5712–5719.
(48) Vidgren, J.; Liljas, A.; Walker, N. P. C. Refined Structure of the Acetazolamide Complex of Human Carbonic Anhydrase II at 1.9 Å. *Int. J. Biol. Macromol.* **1990**, *12*, 342–344.
(49) Sippel, K. H.; Robbins, A. H.; Domsic, J.; Genis, C.; Agbandje-McKenna, M.; McKenna, R. High-Resolution Structure of Human Carbonic Anhydrase II Complexed with Acetazolamide Reveals Insights into Inhibitor Drug Design. *Acta Crystallogr., Sect. F: Struct. Biol. Commun.* **2009**, *65*, 992–995.
(50) Huth, S. W.; Oakley, J. V.; Seath, C. P.; Geri, J. B.; Trowbridge, A. D.; Parker, D. L.; Rodriguez-Rivera, F. P.; Schwaid, A. G.; Ramil, C.; Ryu, K. A.; White, C. H.; Fadeyi, O. O.; Oslund, R. C.; MacMillan, D. W. C. μMap Photoproximity Labeling Enables Small Molecule Binding Site Mapping. *J. Am. Chem. Soc.* **2023**, *145*, 16289–16296.